Appl. Phys. B 58, 197–209 (1994)

Applied Physics B Lasers and Optics

Ultrashort-Pulse Sources Based on Single-Mode Rare-Earth-Doped Fibers

M. E. Fermann

IMRA America, Inc.,1044 Woodridge Avenue, Ann Arbor, MI 48105, USA (Tel.: +1-313/930-2560, Fax: +1-313/930-9957)

Received 21 June 1993/Accepted 19 November 1993

Abstract. An overview of ultrashort-pulse sources based on single-mode rare-earth-doped fibers is given. A wide range of pulse-generation schemes comprising mode-locked fiber lasers, parametric pulse sources and hybrid diode-fiber amplifier sources are discussed. Both actively and passively mode-locked fiber lasers are described and their specific merits and operation regimes are elucidated. Techniques for improving the spectral quality and the output powers of diode-based systems based on amplification in rare-earth-doped fibers are also reviewed. Finally, applications are discussed and directions for future research are indicated.

PACS: 42.60.Da, 42.60.Fc, 42.80

Rare-earth-doped fiber lasers were one of the first laser systems to be described and were developed by Snitzer in 1961 in his pioneering work on glass lasers [1]. In this early work multi-mode fibers were used to alleviate the problems of thermal heating of the glass host and to enable efficient pumping with flash lamps. However, apart from some limited applications in the field of ultrahigh-power lasers, glass lasers did not find wide-spread applications due to a lack of compatibility with available pump sources. Only when Poole et al. [2] succeeded in incorporating rare-earth-ions into *single-mode fibers*, the advantages of glass-fiber lasers became apparent. Apart from the complete elimination of thermal loading, fiber lasers allow operation in a confined diffraction-limited mode, excellent compatibility with single-mode diode pump lasers, long interaction lengths for the laser light in the fiber and very large gain bandwidths. These unique features subsequently led to a revolution in optical technology, the consequences of which we are still witnessing. Particularly noteworthy is the demonstration of the erbium-doped optical amplifier [3] in 1987, which has greatly improved the transmission rates of fiber-based communication systems and has also enabled the demonstration of practical soliton communication systems [4]. Today rare-earth-doped fibers are one of the most widely used solid-state laser media.

The early work on rare-earth-doped fibers was concerned with the improvement of cw glass laser performance [5], taking advantage of the single-mode fiber geometry. Equally, in this period it was realized that rare-earth-doped fibers can serve as attractive pulse sources, but the early emphasis was put on Q-switched fiber lasers delivering ns pulses [6]. Though mode locking in fiber lasers was demonstrated as early as 1986 [7], the operation was flawed due to intracavity reflections at the fiber end faces and pulse widths shorter than 1 ns were not obtained. 100 ps pulses were obtained by several groups in 1988 [8, 9], but initially little was known about the quality of the pulses.

Well-defined mode locking was not demonstrated until 1989, when Phillips et al. obtained 20 ps pulses from a Nd-doped fiber laser [10]. Equally in 1989 soliton-shaping was first used by Kafka et al. to push the pulse widths below the 5 ps mark [11]. Subpicosecond pulses were first obtained in 1990 in an actively mode-locked Nd-doped fiber with additional soliton shaping [12]. 100 fs pulses were first obtained in 1991 in the first truly passively mode-locked fiber laser [13]. At the same time parallel work performed by Duling on monolithic cavity designs led to the demonstration of the first self-starting passively mode-locked fiber laser [14]. The current record for the shortest pulses from a fiber laser lies at 32 fs obtained by Ober et al. in 1993 [15]. However, pulse spectra broader than 70 nm were observed in passively mode-locked fiber lasers early on [16] and in view of the $\approx$50 nm bandwidth of neodymium-silica glass, we can expect that pulses shorter than 20 fs should be eventually generated directly from fiber lasers. These pulse widths are comparable to the performance obtainable with both passively mode-locked dye [17] and Ti:Sapphire lasers, where pulse widths as short as 10 fs have been produced [18]. Thus, fiber lasers truly qualify as ultrafast pulse sources.

The unique features of fiber lasers offer many advantages over solid-state lasers and allow for a much larger range of pulse generation schemes and applications. In particular, the possible very long interaction lengths for weak nonlinear processes may be efficiently exploited for a variety of ultrafast optical devices unknown in the field of conventional

solid-state lasers. A straightforward application of nonlinear processes is the use of the nonlinear phase perturbation induced by an external optical modulating pulse train launched into the fiber laser to produce the all-optical equivalent of AM [19] or FM [20] mode locking. Alternatively, the nonlinear phase modulation induced by a mode-locked pump laser may be used for the synchronization of a master pump laser to a fiber slave laser [21]. These techniques allow the demonstration of all-optical clock recovery [22], all-optical signal regeneration [23] and all-optical clock distribution [21], which are key components of future ultrahigh bit-rate communication systems.

Equally, weak nonlinear parametric processes can be efficiently exploited to produce pulse trains without resorting to an oscillator. Well-separated soliton pulses at repetition rates exceeding 100 GHz were recently so generated in a long length of nonlinear fiber using only the beat signal from two narrow-line cw sources as a seed [24].

Fiber lasers may also be used effectively to amplify pulses from low-power ultrashort semiconductor-laser pulse sources, and thus hybrid diode-fiber systems can be manufactured. Hybrid diode-fiber systems offer unique opportunities for compact high-repetition-rate pulse sources for current soliton communication systems [25]. In a different configuration rare-earth-doped fibers may be used to amplify strongly chirped diode oscillator pulses [26]. Recompression of the pulses after the fiber amplifier can thus produce a very compact hybrid diode-fiber high-power pulse source.

Finally, the high gains achievable with fiber lasers allow passive mode locking with semiconductor saturable absorbers [27]. Semiconductor saturable absorbers typically induce a large linear loss into the cavity, which can prevent lasing altogether in low-gain bulk lasers. Fiber lasers on the other hand offer the advantage of combining advanced semiconductor-growth technology with state-of-the-art fiber technology for the construction of monolithic polarization-insensitive compact pulse sources [28].

1 Active Mode Locking

Active mode locking of fiber lasers is currently the preferred technique for high-repetition-rate pulse generation for communication systems. In active mode locking the pulses are generated in synchronism to a well-defined rf modulation signal, which can also be distributed to a bit-pattern generator for synchronized information encryption onto the pulse train.

A typical arrangement for an actively mode-locked fiber laser is shown in Fig. 1. Particularly when low-dispersion fibers such as erbium-doped fibers emitting at 1.55 μm are used, a completely integrated ring-cavity can be constructed for signal generation. The round-trip fiber length employed is typically less than 10 m, which is also convenient for handling purposes. To avoid polarization drifts, polarization-maintaining fibers can be employed throughout the loop [29]. Mode competition between counterpropagating waves and different polarizations is avoided by a polarizing isolator. Using this type of arrangement and a fast electro-optic modulator, stable pulse trains at repetition rates up to 30 GHz have been generated [29, 30].

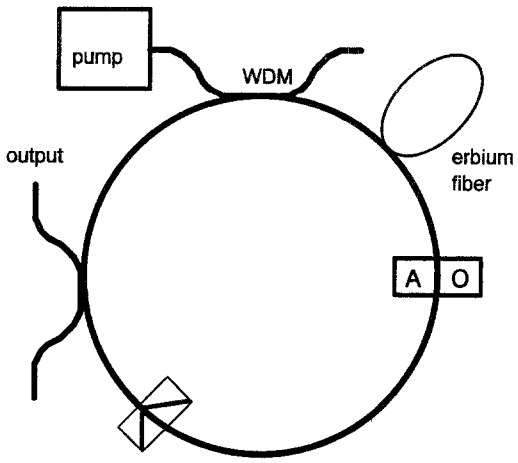

Fig. 1. Cavity design of an all-fiber active mode-locked erbium-fiber laser. WDM is a differential fiber coupler. AO is a modulator

Actively mode-locked fiber lasers are accurately described by mode-locking theory for homogeneously-broadened gain media [31]. In general, either Amplitude (AM) or Frequency (phase) Modulation (FM) is used. Typically, the time-varying modulation exerted by the modulator onto the signal amplitude may be cast into the form

$$M(t) = \exp[-(\delta_a - i\delta_p)\omega_m^2 t^2/2], \quad (1)$$

where $\omega_m = 2\pi f_m$ and f_m is the optical modulation frequency. $\delta_{a/p}$ are the amplitude and phase modulation indices, respectively. δ_p is simply the exerted peak phase retardation in the fiber. For pure FM mode locking, chirped Gaussian-shaped pulses with a FWHM of

$$\Delta\tau = 0.45\left(\frac{2g}{\delta_p}\right)^{1/4}\left(\frac{1}{f_m \Delta f_a}\right)^{1/2} \quad (2)$$

are obtained. In this Δf_a is the bandwidth of the gain medium, g is the saturated intensity gain in the cavity. The time-bandwidth product in this case is $\Delta\tau\Delta f = 0.63$. The time-bandwidth product for bandwidth-limited Gaussian pulses is $\Delta\tau\Delta f = 0.44$ and therefore FM modelocking produces quite strongly chirped pulses. To describe the case of pure AM modelocking, δ_p has to be replaced by δ_a in (2). The resulting pulses are also of Gaussian shape and are bandwidth limited. Note that (2) is valid both for fundamental and higher-harmonic mode locking, where more than one pulse oscillates in the cavity.

Typical modulation indices for standard electro- and acousto-optic modulators are of the order of one. Using the value of 44 nm for the bandwidth of erbium silica fiber [32] we obtain $\Delta f_a = 5.5$ THz. Assuming a modulation frequency of 20 GHz and assuming values of $2g/\delta_p$ of the order of unity, we can expect to generate pulses as short as 2 ps. Pulses as short as 3 ps have recently been produced at this repetition rate [29].

Due to the long interaction length of the signal with the gain medium in single-mode fibers, the pulses typically get distorted by self-phase modulation. The phase modulation exerted by a pulse on itself in a fiber of length l may be written as

$$\Phi(t) = \gamma P l S(t), \quad (3)$$

where P is the peak power and $S(t)$ is the pulse power as a function of time normalized to one. $\gamma = 2\pi n_2/A\lambda_s$ is the nonlinearity parameter of the fiber at the signal wavelength λ_s. n_2 is the nonlinear refractive index, where $n_2 = 3.2 \times 10^{-20}\,\mathrm{m^2/W}$ in typical silica fiber. A is the area within the 1/e-radius of the radial intensity-distribution of the signal light in the fiber. For typical fiber parameters A may be approximated by the core area. Assuming a sech^2 pulse shape, we may write $S(t) = \mathrm{sech}^2(t/\tau)$, where $\tau = \Delta\tau/1.763$ and $\Delta\tau$ is the FWHM of the pulse.

Since the phase modulation induced by self-phase modulation follows a quadratic function near the vicinity of the pulse center, we may define a self-induced complex modulation index according to (1) [33]. For a sech^2 pulse the self-induced modulation index is then calculated as

$$\delta_{sm} = \frac{2\Phi_{nl}}{\omega_m^2\tau^2}\,, \tag{4}$$

where $\Phi_{nl} = \gamma PL$ is the peak nonlinear phase delay in the round-trip fiber length L. Assuming a nonlinear phase delay of $\Phi_{nl} = \pi/30$, a modulation frequency of 300 MHz and a FWHM of the pulse of 15 ps, we obtain $\delta_{sm} \approx 600$. Thus even a very small self-phase modulation-induced phase delay produces a modulation index about 10 times higher than possible with the best acousto-optic modulators [34]. As a result, the pulses are expected to be shorter than estimated by linear active mode-locking theory.

However, since the chirp induced by self-phase modulation is highly non-uniform, an excessive amount of nonlinearity in the cavity will lead to pulse break-up and temporally unstable mode-locking solutions [35]. Haus and Silberberg have found that for the case of positive dispersion in the laser cavity self-phase modulation-induced pulse shortening beyond a factor of two is not possible [35]. Their early theoretical prediction is indeed in good agreement with a number of recent experimental results [10, 33, 34].

For the case of negative dispersion, theoretical estimates about the amount of possible pulse shortening are not as clearly defined. However, assuming the limit where δ_{sm} is very much larger than either σ_a or δ_p, stable pulse solutions can be generated when the amount of negative dispersion in the cavity just compensates for the amount of self-phase modulation, i.e. when the fundamental soliton oscillates in the laser. Dispersion-related pulse broadening scales with the dispersive length $z_d = \tau^2/|\beta_2|$ and self-phase modulation scales with the nonlinear length $z_{nl} = 1/\gamma P$, where β_2 is the group-velocity dispersion in the fiber. Oscillation with the fundamental soliton pulse requires $z_d = z_{nl}$. The corresponding pulses have a sech^2 shape with a FWHM width given by

$$\Delta\tau = \frac{3.53|\beta_2|}{\gamma E}\,, \tag{5}$$

where E is the pulse energy. Due to the large possible variations of the fiber dispersion and pulse intensity in the cavity, z_d and z_{nl} can also be subject to large variations. As shown experimentally by Smith et al. [36] and theoretically by Kelly et al. [37], stable pulse formation is then still ensured when the length-scale of these variations is very much shorter than the soliton period, i.e. $L \ll z_s$, where the soliton period is given by $z_s = (\pi/2)\,z_d$. A fundamental soliton power and soliton period may then still be defined if average values for the dispersion and pulse power are assumed. This is commonly referred to as the "average soliton model".

2 Synchronous Mode Locking

Communication systems based on variations of synchronously mode-locked fiber lasers are currently of great interest for ultra-high bit-rate transmission in optical fibers [23]. Synchronous modelocking of fiber lasers is accomplished by induced phase modulation rather than gain modulation, due to the small absorption cross-section of fiber lasers. In this method the modulating pulse from a master laser is used to periodically perturb the phase of a slave laser via cross-phase modulation, where the slave laser is typically pumped with a cw source [20]. By the generation of side-bands the laser modes may then be locked to produce the all-optical equivalent of FM mode locking [20]. By converting the induced phase modulation into an amplitude modulation in an interferrometrically sensitive cavity, the all-optical equivalent of AM mode locking may also be demonstrated [19]. Note that a mode-locked pump laser may serve directly to modulate the fiber slave laser via pump-induced phase modulation [21].

A typical synchronously pumped mode-locked fiber laser cavity is shown in Fig. 2. It is useful to employ two fiber sections [21]. The first long section is undoped and designed to allow an approximate group-velocity match between the pump and signal. The second short section is doped with rare-earth ions to allow efficient absorption of the pump. Assuming a time frame propagating with the signal pulse and a pump pulse very much wider compared to the signal pulse, the phase modulation of the signal in a fiber of length l induced by a single pump pulse may be written as [38]

$$\Phi(t) = \frac{\gamma_r P\tau_p}{\Delta\beta}\left\{\tanh(t/\tau_p) - \tanh\{(t-\Delta\beta l)/\tau_p\}\right\}, \tag{6}$$

where for simplicity we again assumed a sech^2-pump pulse with a FWHM of $\Delta\tau_p = 1.763\tau_p$. $\Delta\beta = 1/v_{gp} - 1/v_{gs}$ is the difference between the inverse group-velocities at the pump and signal wavelengths $\lambda_{p,s}$. $\gamma_r = 2\pi n_2/A_{p,s}\lambda_s$, where $A_{p,s}$ is the overlap integral between the pump and signal light, which is approximately equal to the core area. Casting the phase modulation into the form of (1), we can again define a complex modulation index. It may then be shown [21] that the modulation index is maximized when $\Delta\beta L = 1.316\tau_p$, i.e. when the length of the modulating fiber is approximately matched to the walk-off length $\Delta\tau_p/\Delta\beta$ between the pump

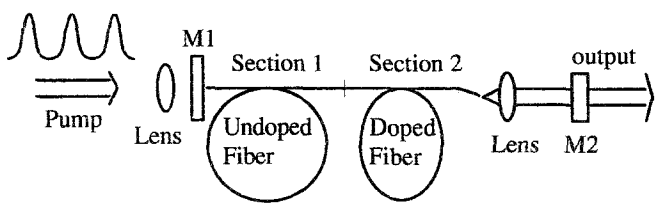

Fig. 2. Cavity design of a synchronously pumped mode-locked erbium-fiber laser

and signal. The maximum possible modulation index is then evaluated as

$$\delta_{\max} = \frac{1.54}{\omega_m^2 \Delta\beta \tau_p} \gamma_r P . \tag{7}$$

In contrast to self-phase modulation, cross-phase modulation does not produce a nonlinear chirp variation in the signal pulse. Instead, the nonlinear chirp variation occurs on the time scale of the pump pulse, which is typically very much longer than the signal pulse. Therefore the induced chirp across the signal pulse will be very nearly linear and no pulse-break up will occur. The induced frequency chirp can be compensated intracavity in fibers with negative group-velocity dispersion and chirp-free pulses can be readily generated [20]. $\delta_{\max}$ can exceed a value of 10,000, which is very much larger than the modulation indices of the order of unity possible with acousto-optic modulators [34]. Therefore, from (2) we may find that all-optical FM mode locking can produce pulses at least an order of magnitude shorter than possible with standard bulk optical modulators. This was verified in a recent experiment where, employing 70 ps pump pulses, chirped 3.6 ps signal pulses were generated at a repetition rate of 100 MHz [21]. The use of 10 ps pump pulses should allow a further shortening of the signal pulses below the ps mark.

Synchronous mode locking can therefore produce pulses nearly as short as possible with passive mode-locking techniques. In addition, since no interferrometrically sensitive cavity components are required, an environmentally stable cavity may be constructed by resorting to polarization-maintaining fiber components. Synchronous mode locking may further be used for all-optical clock recovery [22]. In clock recovery an external modulating pulse train is used that contains both ones and zeros. Since on average the fundamental carrier frequency of this bit-pattern is still defined, it may be used to synchronously mode-lock a fiber laser. To this end only all-optical FM mode locking may be applied, since no loss is introduced outside the location of the ones. In an additional application of synchronous mode locking, all-optical signal regeneration has also recently been demonstrated [23]. In this, the pulse train containing the bit pattern is reused to modulate the recovered clock; and therefore a retimed and reshaped bit pattern is generated. Clearly, these techniques offer a great potential for all-optical signal processing in future ultrahigh-capacity communication systems.

3 Kerr-Type Passive Mode Locking

3.1 Basic Cavity Designs

Kerr-type passive mode locking is the preferred technique for the generation of the shortest possible pulses, since it allows to take advantage of the full bandwidth of fiber lasers. In most Kerr-type mode-locked systems self-phase modulation dominates the pulse formation process. However, in contrast to active mode locking, an amplitude modulation mechanism coexists on the time scale of the oscillating pulse, which ensures pulse-stability even in a highly nonlinear cavity.

Due to the near-instantaneous response of the Kerr-nonlinearity, we may assume a near-instantaneous amplitude modulation in the fiber. This is conveniently described by introducing a nonlinear reflectivity of one of the two cavity mirrors of a fiber laser, which for small pulse powers may be written as

$$R_{nl} = R_0 + \kappa P , \tag{8}$$

where κ is a constant.

Steady-state pulse formation in the cavity is obtained when a given pulse solution differs from itself by only a constant phase shift after one round trip. This is conveniently written in form of an operator equation, i.e.

$$\hat{T}(z) V_n(t,z) = e^{i\psi} V_n(t,z) , \tag{9}$$

where $V_n(t,z)$ is the pulse envelope as a function of time and position in the cavity and $\hat{T}(z)$ is a differential transfer operator representing the pulse-shaping elements in the cavity. In Kerr-type mode-locked fiber lasers, the operator equation may be written to first order as [39–42]

$$\frac{i}{2} D_2 \frac{\partial^2}{\partial t^2} V + \frac{1}{2}(g-\alpha)V - i\gamma L(1+i\varepsilon)|V|^2 V = i\psi V , \tag{10}$$

where α is the intensity loss coefficient, $D_2 = \beta_2 L$ is the total average dispersion in the fiber and ψ is the phase-shift per round-trip. Note that we have neglected a bandwidth limitation from the gain medium, which is a valid approximation for most passively mode-locked fiber lasers. γ governs passive phase modulation in the fiber and $\varepsilon\gamma$ governs the passive amplitude modulation. κ is related to $\varepsilon\gamma$ by $\kappa = \varepsilon\gamma L$. In most passively mode-locked Kerr-type systems $\varepsilon \ll 1$ and thus pulse formation may still be described by an average soliton model. The observed pulse widths thus correspond to the soliton pulse widths in (5). However, (10) contains no information on possible pulse-shape variations in the cavity and is therefore accurate only when the pulse-shaping cavity elements are distributed evenly along the fiber, i.e. when the cavity is constructed entirely from negative dispersion fiber. In the presence of large dispersive perturbations a better description of the pulse formation may be obtained by resorting to the solitary laser model [43–45], i.e. by incorporating higher-order terms in the expansion of the transfer operator.

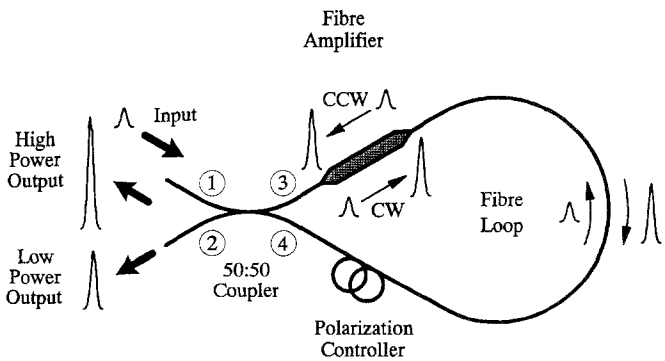

Fig. 3. Operation principle of a NALM operated in reflection

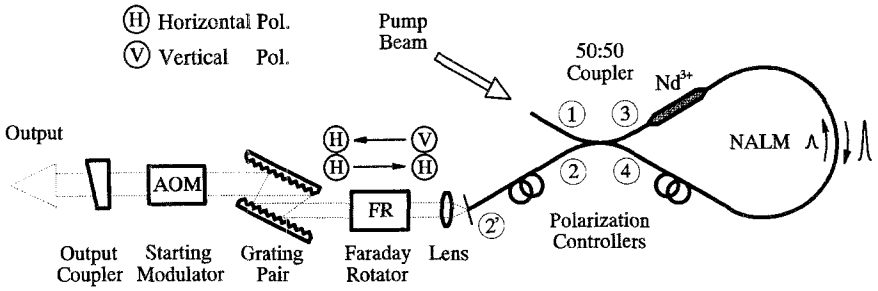

Fig. 4. Cavity design of a Nd-fiber laser Kerr-type mode-locked with a NALM

Though Kerr-type mode-locking of fiber lasers has been known for some time [13, 14, 16], the general interest has focused on two systems. The first system employs a Nonlinear Amplifying Loop Mirror (NALM) [46, 13, 14], as shown in Fig. 3. When the polarization state is preserved in the fiber loop it is completely reciprocal and will act as a perfect mirrorr [47]. The linear reflectivity can simply be changed by rotating the polarization state by 90° somewhere in the loop. Clearly, the polarization rotation breaks the symmetry of the loop, since sections of the loop will be traversed by counterpropagating waves of different polarization states. Therefore, the linear phase delay φ between the two waves can then be adjusted by suitable polarization controllers. A reflectivity change as a function of intensity can be obtained by an uneven power splitting in the coupler [48] or by placing a gain medium asymmetrically inside the loop, as is the case for the NALM [46]. Self-phase modulation thus causes different nonlinear phase shifts for the two counterpropagating waves and hence any reflected or transmitted pulse will be amplitude modulated. The operation principle of a NALM is further elucidated in Fig. 3.

The cavity design of a Nd fiber laser passively mode-locked with a NALM operated in reflection [13] is shown in Fig. 4. The system employed an acousto-optic modulator for pulse start-up and allowed the generation of 100 fs pulses from a fiber laser for the first time. Recently most of the interest has focussed on monolithic Er lasers passively mode-locked with a NALM operated in transmission as first demonstrated by Duling [14]. Since this type of cavity resembles a figure of eight, it is commonly referred to as the Figure of eight Laser (F8L). Neglecting the amplifier length and fiber lengths outside the Sagnac interferometer, the NALM system can be characterized by a value of κ of [49]

$$\kappa = -\gamma L \frac{g-1}{g} \sin 2\phi\,, \tag{11}$$

where 2φ is an arbitrary linear phase-delay between the clockwise and counter-clockwise propagating pulses in the NALM. κ is maximized when $\varphi = -\pi/4(\pm n2\pi)$. Note that in this system the amount of passive phase modulation can equal the amount of passive amplitude modulation. However, to date even in the NALM system no significant departure from the average soliton model was found, may be due to the unavoidable long fiber leads in the NALM.

The operation principle of the second system is shown in Fig. 5 [16]. Here nonlinear polarization evolution in a weakly linearly birefringent fiber [50, 51] is employed for passive amplitude modulation. In a standing-wave cavity the

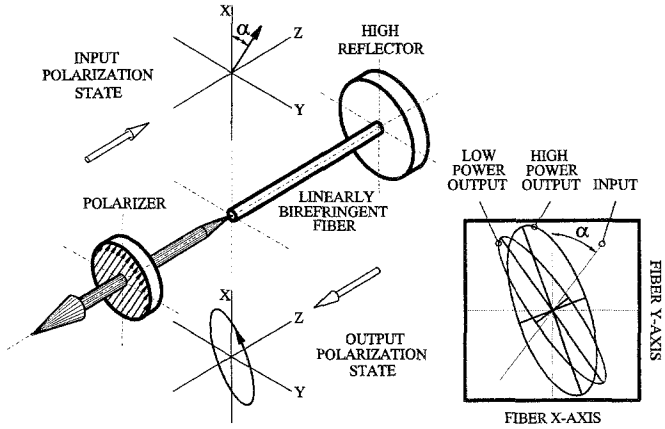

Fig. 5. Operation principle of nonlinear polarization evolution as used for Kerr-type mode locking

value for κ is obtained as [49, 52]

$$\kappa = -\frac{\gamma L}{12} \sin 4\phi \sin 2\phi \sin 2\varphi\,, \tag{12}$$

where ϕ is the angle of orientation of the linearly polarized eigenmodes of the fiber with respect to the intra-cavity polarizer and φ is the round-trip phase delay along the two polarization axes. Recent experiments [52] have indeed shown that even in the presence of large dispersive perturbations this system operates with a passive amplitude modulation coefficient ε (10) as small as 0.02.

3.2 Self-Starting Criteria

The potential of these systems to start mode locking from noise may be inferred from measurements of the mutual coherence time τ_c of the axial modes in the cavity [53]. τ_c is related to the inverse of the half width of the first beat note of the oscillating cavity modes in the free-running laser by $\tau_c = 1/\pi\Delta\nu_{3dB}$. Self-starting may then be obtained when the critical build-up time T_{crit} of a pulse in the cavity is shorter than τ_c, where $T_{crit} = T_R/\kappa\bar{P}_{cw}\ln(m)$. T_R is the round-trip cavity time, $\bar{P}_{cw}$ is the average intracavity power and m is the number of initially oscillating cavity modes. In a perfect cavity all modes would be evenly spaced and $\Delta\nu_{3dB}$ would be infinitely narrow. In real systems, $\Delta\nu_{3dB}$ has typical widths ranging from 1 kHz to 1 MHz. The dominant mechanisms for the beat-note broadening arise from spurious cavity reflections [54] and gain gratings resulting from spatial hole-burning in the fiber [55], which cause uneven

frequency shifts of the oscillating cavity modes. Whereas beat-note broadening due to cavity reflections may be reduced to less than 2 kHz in well-designed fiber lasers [15], beat-note broadening due to frequency shifts arising from gain gratings is often unavoidable and can be the dominant mechanism preventing self-starting of fiber lasers [15, 55].

The most efficient way to suppress spurious cavity reflections and thus beat-note broadening is in a ring cavity, where, to first order, intracavity reflections are absorbed by the intracavity isolator and only doubly-reflected waves cause uneven frequency shifts. Particularly suitable is an erbium fiber ring cavity, where nonlinear polarization evolution may be readily employed for passive amplitude modulation. Such a system was first demonstrated by Matsas et al. [56] and later improved by Tamura et al. [56], who constructed the first passively mode-locked Kerr-type fiber system that self-started with a single pulse in the cavity.

3.3 Environmentally Stable Cavities

The disadvantage of ring-cavity designs is the unpredictability of the polarization control, which has to be incorporated to adjust the phase delay φ between the two polarization axes in the fiber. Since the phase delay is interferometrically sensitive to temperature variations and environmental perturbations, a continuous adjustment of the polarization control is required. In the absence of pressure variations in the fiber (as induced by fiber coiling) a very stable passively mode-locked erbium ring laser may be constructed with ultra low birefringence fiber [58]. In this case no birefringence is contributed from the optical fiber and therefore a phase delay induced by other (bulk) cavity elements can be preserved indefinitely. It appears that the laser can even work with a negligible linear phase delay and 100 fs pulses were recently so generated.

A continuous phase control is acceptable provided it is reproducible. Such a system was recently demonstrated by resorting to a special form-birefringent rectangular fiber design as shown in Fig. 6, where nonlinear polarization evolution was used for passive amplitude modulation. In a standing-wave fiber cavity, a polarizer can permanently fix the angle ϕ, whereas the phase delay φ along the two axes may be set by a single piezo-electric element that applies a continuously adjustable amount of pressure to the flat side of the fiber [59]. Continuous single-pulse oscillation may then be ensured by either synchronous pumping [21, 59] or by a continuous slow movement of one of the cavity mirrors [15, 60].

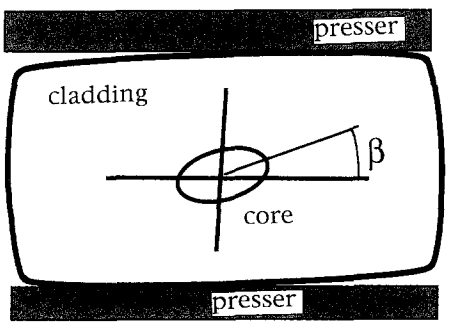

Fig. 6. Cross section of a weakly form-birefringent polarization maintaining fiber for environmetally stable Kerr-type mode locking using nonlinear polarization evolution

Recently, the continuously adjusted phase controller was eliminated [61] by using a Faraday rotator mirror [62] at one end of the cavity. The Faraday rotator mirror rotates the polarization of the reflected light by 90° with respect to the incoming light and therefore the light propagates backward down the fiber in exactly the orthogonal polarization state. Hence the total linear phase delay between the polarization eigenmodes of the fiber is exactly zero after one round trip. On the other hand, nonlinear phase changes remain uncompensated and accumulate along the polarization eigenmodes after reflection off the Faraday mirror. The polarization rotation induced by the Faraday mirror is readily compensated by the inclusion of a second Faraday rotator and an environmentally stable linear phase delay is incorporated by including a bulk wave plate into the cavity. The fiber in this system may be coiled and pulses as short as 125 fs were recently so generated with an erbium fiber laser [61].

Finally, a F8L was recently constructed by resorting to highly-birefringent fiber in all cavity components [63]. Since this cavity is polarization-maintaining, a linear polarization state is preserved in all sections of the fiber laser. As a result, the fiber loop is perfectly reciprocal and not interferometrically sensitive, i.e. in linear operation all the light is reflected by the fiber loop. Light transmission through the loop is then obtained by simply using an unequal splitting ratio in the loop coupler. Clearly,the disadvantage of this design is that $\kappa = 0$. Hence, long fiber lengths and high pump powers have to be used to start up pulse oscillation, which also prevents self-starting of the system with a single pulse in the cavity.

3.4 Departures from the Average Soliton Model

The tendency of Kerr-type mode-locked fiber lasers to oscillate with more than one pulse in the cavity at elevated pump powers may be understood from the nonlinear response of the reflectivity function in (8) and also the departure of a mode-locked fiber laser from the average soliton model. The interferometric sensitivity of the cavity designs employed for Kerr-type mode locking leads to a sinusoidal response of the nonlinear reflectivity function in (8) on pulse power and thus a decrease in reflectivity for high pulse powers. In practice this point is never reached, since the pulses then start to break up into pulse bunches with a corresponding decrease in pulse power. Due to this saturation mechanism, the pulse energy in typical Kerr-type passively mode-locked fiber lasers is approximately "quantized" [64, 56], i.e. a plot of the laser output power versus pump power shows discrete steps corresponding to the addition of single pulses to the cavity. A measurement taken of soliton "quantization" from [64] is reproduced in Fig. 7.

The departure of the laser from the average soliton model is also instrumental in limiting the power of the pulses, as pointed out by several authors [65, 66]. As the energy of the pulses grows, the pulses shorten and give rise to a decrease in the soliton period. As the soliton period approaches

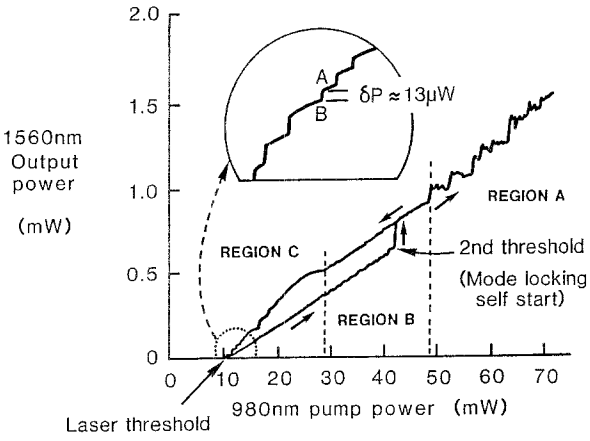

Fig. 7. Average output power vs input power measured in a Kerr-type mode-locked erbium-fiber laser [64]. The discrete steps in the insert correspond to the addition of single oscillating soliton pulses to the cavity

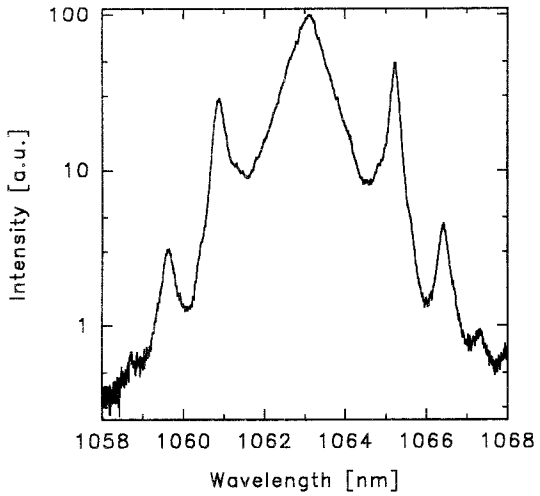

Fig. 8. Resonant spectral side bands in an active-passive mode-locked Nd-fiber laser [69]

the cavity length, the pulses get formed appreciably by each cavity element. Without adiabatic transformations, non-soliton parts coexist with the main pulses in the cavity elements. These non-soliton parts are shed continuously into a dispersive wave that co-propagates with the soliton [67]. The dispersive wave propagates at a different phase velocity form the soliton and can only couple resonantly to the soliton when the wavenumber difference is made up by the periodicity of the pulse perturbations [67]. Assuming a perturbation periodicity on the scale of the cavity length L, the phase matching condition is obtained as $k_s - k_d = 2\pi N/L$, where $k_s = 2\pi/8z_s$ is the wave vector of the soliton and $k_d = \beta_2 \Delta\omega^2/2$ is the wave vector of the dispersive wave. As a result, resonant side bands appear on both sides of the soliton spectrum. From the phase-matching condition the separation of the side bands from the center of the soliton frequency is obtained as

$$\Delta\Omega_n = \pm\frac{1}{\tau}\sqrt{-1+\frac{8Nz_s}{L}}, \tag{13}$$

as first derived by Kelly [68]. Spectral side bands were first observed by Hofer et al. [34] and Fermann et al. [69] in an active-passive mode-locked Nd-fiber laser and later by Richardson et al. [70] in a Kerr-type mode-locked Er fiber laser, but they were not correctly explained until 1992 in the work by Pandit et al. [71]. The early measurement from [69] is reproduced in Fig. 8. A subsequent analysis by Hofer [72] has shown that the positions of the side bands are indeed in good qualitative agreement with (13).

Resonant coupling between the dispersive wave and the soliton is proportional to the spectral intensity of the soliton at the side band location [67]. Numerical studies performed by Matsas et al. [65] have shown that the soliton becomes unstable when the location of the side bands falls within the main part of the soliton spectrum, i.e. when $z_s/L \leq 0.3$. From this condition Matsas et al. [65] have derived a limiting expression for the shortest soliton pulse width possible in passive Kerr-type mode-locked systems

$$\tau_s \geq 0.75\sqrt{\beta_2 L}. \tag{14}$$

Equation (14) is in good agreement with most published reports on Kerr-type passive mode locking in Er fibers down to pulse widths of 100 fs, which are typically the shortest pulses obtained directly from Er fiber lasers [60].

3.5 Solitary Fiber Lasers

The average soliton model becomes less appropriate in the case of large dispersive perturbations as encountered in a fiber laser, where bulk optical components are used for dispersion compensation [13, 15, 16, 52]. An example of such a cavity design was shown in Fig. 4. In these systems

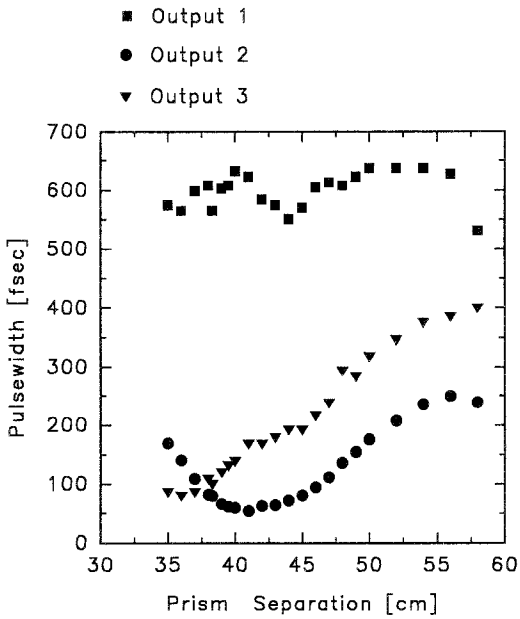

Fig. 9. Intracavity pulse-width variations in a dispersion-compensated (as in Fig. 4) Kerr-type mode-locked Nd-fiber laser [52]. Output 1, 2, and 3 are the pulse widths measured before, in the middle of, and after the intracavity dispersive delay line, respectively. The shortest pulses are observed at output 2, the dispersive end of the cavity

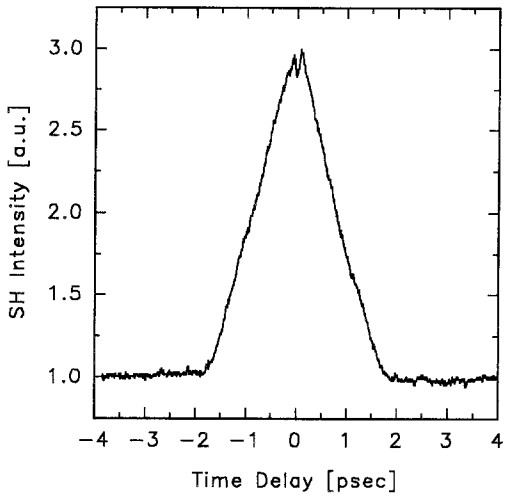

Fig. 10. Colinear autocorrelation trace [52] of strongly chirped nearly rectangular pulse generated at output 1 (as in Fig. 9)

pulse-width variations of more than one order of magnitude can be encountered intra-cavity. An example taken from [52] is shown in Fig. 9, where the pulse widths at different points in the cavity were measured. The shortest pulses were observed at the dispersive end of the cavity (e.g. the output end in Fig. 4) and were approximately bandwidth limited. Strongly chirped pulses were measured at the intracavity fiber end (e.g. coupler output port (2) in Fig. 4). The pulses generated at the intracavity fiber end can greatly deviate from a sech^2 form and can even approximate a rectangular shape [52], as shown in Fig. 10. Note that strongly chirped pulses can be used to limit the nonlinearity of the cavity to enable mode-locked oscillation with increased pulse energies [52]. This technique was recently used in a Kerr-type mode-locked Nd fiber to provide seed pulses for a bulk glass Nd amplifier [73]. Recently, Tamura et al. [74] have succeeded in constructing a very interesting all-fiber derivation of this technique. In this strongly chirped pulses in a cavity with balanced amounts of positive and negative dispersion fiber are used to lower the intracavity peak pulse power and to increase the output pulse energy by one order of magnitude compared to a system with only negative dispersion fiber.

The average soliton model cannot explain these effects, since it assumes small pulse shaping per cavity element and essentially a constant pulse width inside the cavity, i.e. $z_s \gg L$, a soliton period very much longer than the cavity length. Information about the variation in pulse width and chirp can be obtained by resorting to the "solitary-laser" model developed by Brabec et al. [43, 44] and Krausz et al. [45]. In this, large pulse shaping in the cavity elements is assumed, which leads to a position-dependent transfer operator (9). As a result, the steady-state pulse solution also becomes position dependent.

In particular, the solitary laser model shows that approximately bandwidth-limited pulses are obtained only at the opposite ends of a Fabry-Perot cavity. Inside the cavity the pulses are strongly chirped, where the pulse chirp is anti-symmetric with respect to the direction of pulse propagation. The shortest pulses are obtained at the dispersive end of the cavity, since in this case self-phase modulation acts prior to (negative) group-velocity dispersion, which leads to intra-cavity pulse compression [75]. Note that on the backward path the dispersion-compensating cavity elements generate a negatively chirped pulse. The subsequent action of self-phase modulation thus leads to spectral narrowing and an increased pulse width at the other end of the cavity.

The observation of intracavity pulse compression in Kerr-type mode-locked systems was first made by Hofer et al. [34] and later modeled numerically by Fermann et al. [12, 13]. In the case of overall negative dispersion in the laser cavity, the framework of the solitary-laser model predicts a FWHM pulse width at the dispersive end of the cavity of

$$\Delta\tau = \frac{3.53|\beta_2|}{\gamma E} + 0.1\gamma LE\,, \tag{15}$$

as first derived by Brabec et al. [43]. Numerical studies have shown [44] that (15) is accurate even for a highly nonlinear cavity, to within the limit $z_s/L \geq 0.1$. A good agreement of (15) with experiments was found in recent work [76].

3.6 High-Harmonic Mode Locking

One limitation of Kerr-type mode-locked fiber lasers is that they do not easily lend themselves to oscillation at very high repetition rates as required for applications in the telecommunications area. The highest fundamental repetition rate obtained from Kerr-type mode-locked fiber lasers is currently still as low as 100 MHz [60], which corresponds to a cavity length of 3 m. Long cavity lengths arise either from the requirement of dispersion compensation in Nd-doped fibers or the low absorption cross-sections and the low doping levels possible with Er ions. A possible solution around this problem may be the incorporation of sub-cavities that can fix the repetition rate at a much higher value, as demonstrated by Harvey et al. [77] and Yoshida et al. [78]. An example of such a cavity design (reproduced from [78]) is shown in Fig. 11. The major drawback of these systems is that they are sensitive to optical phase fluctuations between the major and the sub-cavity, which makes sophisticated stabilization schemes a necessary requirement [77]. However, experiments have demonstrated that phase-insensitive sub-cavities may also be designed [78, 79], though a detailed

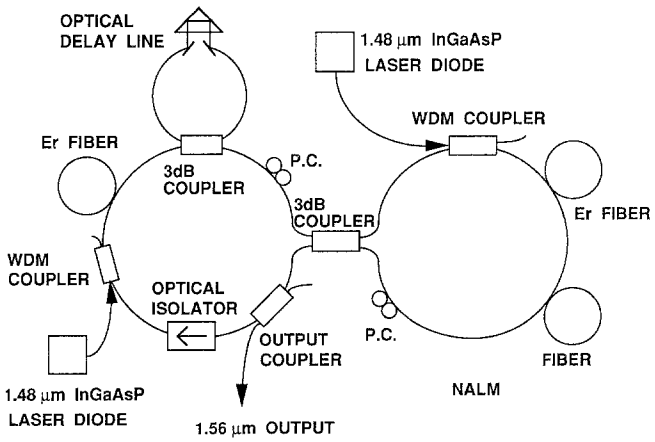

Fig. 11. Kerr-type mode-locked erbium-fiber laser with a sub-cavity for repetition rate control [78]

explanation for the observation of stable higher-harmonic mode-locking has not yet been given.

Another recently described experiment [80] suggests the use of long-range electrostrictional interactions between solitons [81] to obtain passive harmonic mode locking without sub-cavities. Such a method would be attractive, since it is selfstabilizing and non-interferometric in nature [80]. Unfortunately, the electro-strictionally induced repulsive forces between solitons are very weak and therefore practical systems may require special fiber designs that enhance the effect.

4 Passive Carrier-Type Mode Locking

Carrier-Type Mode Locking (CTM) of fiber lasers, as first demonstrated by Zirngibl et al. [27], is currently emerging as the preferred technique for the generation of low repetition rate pulses with widths between 300 fs and a few ps. CTM allows self starting operation (with a single pulse in the cavity) in all-polarization maintaining fiber [82] CTM may be insensitive to polarization drifts in weakly-birefringent fiber [28] and it allows stable operation with negligible self-phase modulation in the cavity [83]. In CTM systems pulse formation is dominated by passive amplitude modulation arising from saturable absorption in a semiconductor near the band edge. The saturation characteristics are determined by the carrier life time (10 ps to 30 ns [84]), and a time constant of ≈300 fs arising from exciton screening [85] and carrier thermalization [86]. For pulses shorter than these time-constants and for a cavity round-trip time very much longer than the relaxation times, the absorption saturates as a function of pulse energy in the form

$$\alpha = \sum \frac{\alpha_i}{1 + \frac{E_\mathrm{p}}{E_{si}}} + \alpha_{ns}\,, \tag{16}$$

where α_{si} is the saturable absorption due to an absorption mechanism. E_p is the pulse energy density and $E_{si} = h\nu/\sigma_{si}$ is the saturation energy density of the respective saturation mechanism with the absorption cross section σ_{si}. α_{ns} is the non-bleachable absorption. Typical values for the saturation energy densities due to long-lived carriers are of the order of 1 mJ/cm^2 [86, 87] and for the two fast mechanisms saturation energy densities smaller by a factor of three are typically assumed [86]. These values are proportional to the total linear absorption and increase linearly with the ratio of the absorption at the band edge to the absorption at the band tail [86], where mode-locking is typically obtained. The long time constant governs the start-up dynamics and the short constant determines the shortest possible pulse widths.

To date the best performance of a CTM fiber laser [83] has been obtained by using a Multiple Quantum Well (MQW) saturable absorber as part of an anti-resonant nonlinear Fabry-Perot mirror [88]. In this, one reflecting side was made up from a totally reflecting stacked mirror structure and the other reflecting side was simply the front-surface reflection (≈33%) from the MQW. The nonlinear mirror design and the cavity setup used in [83] are reproduced in Figs. 12 and 13. The antiresonant structure reduces thermal loading of the MQW and increases its effective saturation energy. With the cavity design from [83], the self-starting mode-locking threshold was obtained with 15 mW of absorbed pump power at an intracavity pulse energy of 180 pJ, allowing for diode-pumped operation, as also demonstrated in [83]. The corresponding energy density inside the MQW was about 600 μJ/cm^2. Higher pulse energies could be obtained by reducing the focusing onto the MQW.

The pulse energy on the MQW should be comparable to its saturation energy to ensure an appreciable amount of amplitude modulation, which is in accord with the results from [83]. The significance of the results from [83] is further that passive mode locking with an intracavity nonlinear phase delay of only $\pi/7$ was obtained, which demonstrates that passive frequency modulation plays a minor role in the pulse-formation process. As a consequence, the pulse widths are far less sensitive to dispersion as in Kerr type mode-locked systems [83] and the pulse spectrum can be totally free of resonant side bands, as recently confirmed in a CTM Er fiber laser [89].

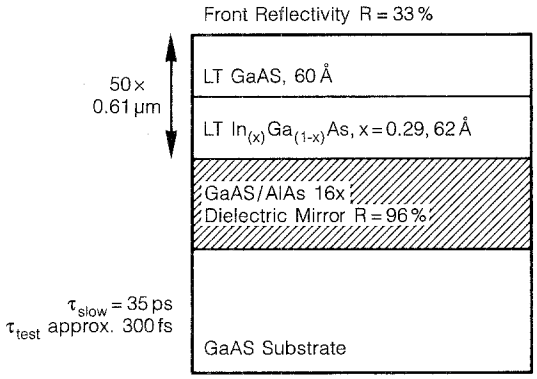

Fig. 12. Anti-resonant Fabry-Perot saturable absorber based on a GaAs/InGaAs multiple quantum well as used for carrier-type mode locking [83]

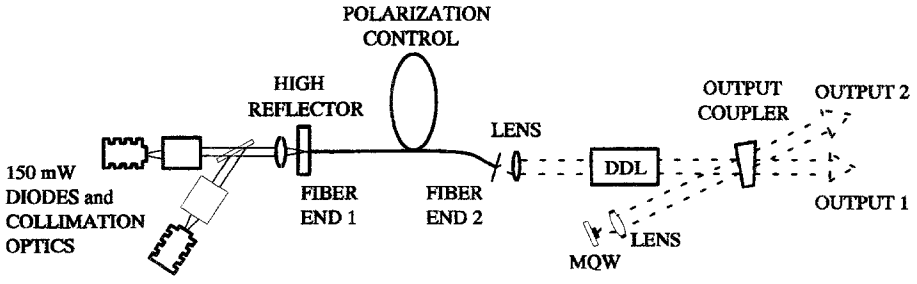

Fig. 13. Cavity design of a diode-pumped self-starting carrier-type mode-locked Nd-fiber laser [83]. DDL is a dispersive delay line

High repetition rate operation in CTM is generally more easily accomplishable than in Kerr-type systems. The two limitations are the high pulse energies required to appreciably saturate the absorbers and the rapid fall-off of the nonlinear responses of the absorbers at high repetition rates [87]. Since CTM-fiber systems are less sensitive to dispersion, no dispersion compensation is required for short lengths of Nd fibers and Nd-fiber oscillators could in principle be operated at a fundamental repetition rate of a few GHz. A Nd-fiber laser could then be used as a master-clock oscillator for the synchronization of an Er/Yb-fiber laser [90]. The incorporation of sub-cavities also provides an opportunity for high repetition-rate pulse generation, as shown by Keller et al. [87], who demonstrated the production of pulses at repetition rates up to 1 GHz in a bulk CTM Nd:YAG system. Here optical phase fluctuations are self-compensating by corresponding fluctuations of the optical carrier frequency. Recently, harmonic partitioning [91] of a CTM-fiber laser was also demonstrated as a viable technique for high repetition-rate pulse generation. In this, the saturable absorber is located asymmetrically within a Fabry-Perot-type cavity, where the round-trip distance from the left cavity mirror to the saturable absorber is chosen to be an n-multiple of the distance from the saturable absorber to the right cavity mirror. The saturable absorber is then optimally bleached when exactly $n+1$ pulses oscillate in the cavity simultaneously and stable higher-harmonic mode-locking may be obtained. This technique is also insensitive to optical phase fluctuations.

5 Parametric Pulse Sources

Parametric pulse sources [24, 92] based on modulational instability in optical fibers are possibly the most attractive candidates for the generation of ultrahigh repetition-rate (>100 GHz) pulse trains. A parametric pulse source comprises one of several classes of oscillator-less pulse sources, as also discussed in the next chapter. It has the unique feature that it allows pulse generation based only on soliton shaping without any passive amplitude modulation.

Parametric pulse sources are based on four-wave mixing between two high-power narrow-band seed signals with a well-defined frequency separation of δf_s in a long optical fiber. Here four-wave mixing substitutes the frequency modulator in active mode locking, leading to the generation of side bands at multiples of δf_s. The phases of the frequency components are self-adjusting and can add up to pedestal-free soliton pulses by adiabatically amplifying the seed signal along the fiber length, as first proposed by Dianov et al. [93]. In contrast to active mode locking (with the exception of opposite phase states in standard FM mode locking) the phases of adjacent pulses are opposite [94]. As a result, the solitons repel each other and are well separated, where mark/space ratios of 10 can be achieved. When launched into long gain-free fibers the soliton pulses are therefore practically non-interacting. The attractive feature of the technique is that it allows tuning of the repetition rate by simply tuning δf_s. In the early experimental demonstrations of this method [24, 92] pulse trains at a repetition rate of 70 GHz have been obtained. Later optimization has allowed the generation of pulse trains with repetition rates between 30 GHz and 50 GHz, which, however, required the incorporation of an additional passive amplitude-modulation mechanism [95].

Mamyshev et al. [94] have identified two necessary conditions for the generation of high-quality soliton pulses. The seed-signal amplitude should be less than the amplitude of a soliton with duration $T/2$, where $T = 1/\delta f_s$ is the beat period of the seed signal. Adiabacity of the amplification process is ensured when $gT^{-2} < 12$, where g is the intensity gain coefficient in the fiber. The final soliton pulse width is calculated from the total energy of the signal after amplification and is given by

$$\Delta\tau = \frac{3.53|\beta_2|}{\gamma \bar{P}_b T G}, \tag{17}$$

where $\bar{P}_b$ is the average power in the beat signal and G is the overall energy gain. Dianov et al. [93] have shown that a total energy gain of 9–18 is sufficient to obtain a mark/space ratio of 10.

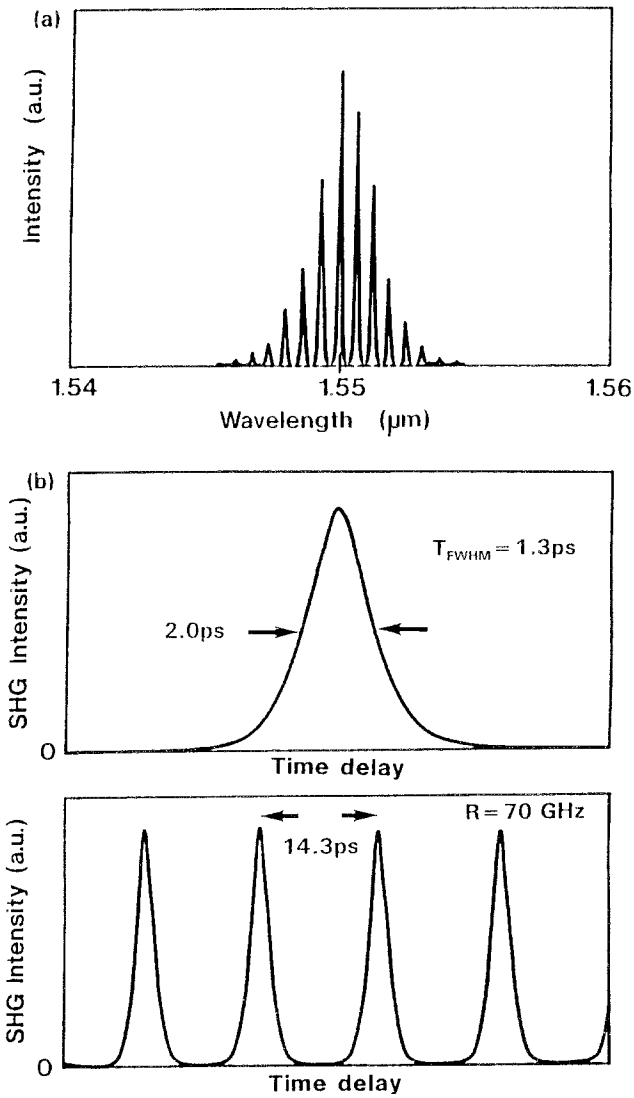

Fig. 14a, b. Spectrum and autocorrelation functions of a 70 GHz soliton train at the output of a fiber with slowly decreasing dispersion [92]. The input beat-signal power was 300 mW

Adiabatic pulse-width shortening cannot only be obtained with signal amplification, but also by an adiabatic reduction of the fiber dispersion along the fiber length. In fact, the two cases are equivalent as may be shown by a linear transformation of the nonlinear Schrödinger equation [93, 94]. Therefore, fibers with slowly decreasing dispersion, i.e. from a value $\beta_2(0)$ to a value $\beta_2(z_f)$ may also be used for high-quality soliton formation. The final pulse width is then still given by (17), where the fiber parameters correspond to the final parameters at z_f and G is replaced by an effective gain coefficient $G_{eff} \approx \beta_2(0)/\beta_2(z_f)$.

The early experimental demonstrations [24, 92] of cw soliton pulse-train generation were all based on the second technique. The beat signal was derived from two distributed-feedback lasers. Since the parametric light sources typically require average seed power levels $\bar{P}_b$ of up to 1 W, the beat signal was amplified in a section of strongly pumped Er-doped fiber. A typical pulse train with a repetition rate of 70 GHz and the corresponding pulse spectrum generated with a beat signal power of 300 mW is shown in Fig. 14 [92].

Currently, no long-distance soliton transmission experiments involving these pulse sources have been performed. Clearly, more work is required to evaluate the practicability of parametric pulse sources in communications. In particular, the encryption of information onto the pulse trains requires all-optical clock-recovery and multiplexing techniques, which are at a very early research stage. In the field of materials studies, where pulse trains at THz repetition rates are required, parametric pulse sources offer an attractive alternative to conventional techniques based on passive frequency filtering [96].

6 Hybrid Diode-Fiber Systems

Hybrid diode-fiber short-pulse sources are probably the most flexible and can be used in a large variety of different configurations for a wide range of applications spanning communications, device testing and optical sensors.

The first class of demonstrated device configurations was a fiber laser comprising both diode and fiber amplifiers [97]. The design allows AM mode locking of the cavity by simply modulating the current to the diode amplifier. An advanced version of this technique [98] was recently employed to generate near-bandwidth-limited 25 ps pulses at a repetition rate of 5 GHz. which is an operation regime attractive for soliton communications. In another method, the current of the diode pumping the fiber amplifier was incorporated into the fiber-laser cavity and the phase variation in the pump laser obtained from modulating the drive current was used for FM mode locking of the fiber laser [99]. However, these techniques do not eliminate nonlinear chirp contributions from carrier excitation in the diode and it is therefore questionable if they can perform well for pulses with widths of less than 10 ps.

Another class of devices is attractive due to its particular simplicity and the possibility of adjustable repetition rates. In this, a high repetition-rate pulse train is obtained from a Gain-switched Distributed-FeedBack (DFB) laser diode. Spectral filtering of the pulses is used to eliminate the nonlinear chirp on the pulses and to minimize their time-bandwidth product. Subsequent amplification in an erbium amplifier can then produce soliton pulses that may be directly used in soliton communication systems [25]. However, a comparison of soliton pulse sources based on this technique and an actively mode-locked erbium-fiber laser by Mollenauer et al. [100] has shown that the residual chirp in gain-switched systems generates additional transmission errors in ultralong-distance soliton communication systems. One possible technique to eliminate this drawback may be to compensate the residual chirp from the spectrally filtered pulses from the DFB laser [101]. However, the added complexity of the system then reduces its practicability.

A final very attractive hybrid system comprises a pulsed wavelength-modulated DFB laser [26] operating at $\approx$1.55 μm. The rapid wavelength modulation of the DFB can impose a very large, nearly linear positive chirp on the 1 ns output pulses. On this time scale the technique allows a wavelength change of up to 10 nm. The pulses can be amplified in an erbium-doped fiber and compressed in a length of negative dispersion fiber. Recent experiments have demonstrated the generation of 200 fs pulses with an energy content up to 2 nJ [102]. The pulse energy is 2 times higher than obtained with any diode or fiber oscillator. The technique is also very attractive since it may potentially allow to reach pulse energies close to the saturation energy of erbium amplifiers (1 μJ) by the application of the chirped pulse amplification technique [103] to optical fibers, as recently demonstrated by Stock et al. [104].

7 Summary

Clearly this short article could not cover all methods for the generation of ultrashort pulses in single-mode rare-earth-doped fibers. I therefore put the emphasis on encountered similarities and differences between the various methods. It was attempted to provide a uniform treatment of the field, but clearly more work is required to improve the understanding of synchronization issues and pulse formation particularly in carrier-type mode-locked systems and in hybrid diode-fiber systems. Nearly a decade after the early research on single-mode rare-earth-doped fiber lasers, they are set to greatly simplify ultrafast optical technology. As a result, applications outside the research environment will soon also become possible.

Acknowledgements. I am indebted to M. Hofer, M. Nakazawa, M.H. Ober and D.J. Richardson for providing me with original figures. I am grateful to R.H. Stolen, M.L Stock and D. Harter for a critical reading of the manuscript. I also acknowledge financial support from the Alexander von Humboldt Stiftung.

References

1. E. Snitzer: Phys. Rev. Lett. **7**, 444 (1961)
2. S.B. Poole, D.N. Payne, M.E. Fermann: Electron. Lett. **21**, 737 (1985)
3. R.J. Mears, L. Reekie, I.M. Jauncey, D.N. Payne: Electron. Lett. **23**, 1026 (1987)
4. M. Nakazawa, K. Suzuki, Y. Kimura: Opt. Lett. **15**, 715 (1990)
5. R.J. Mears, L. Reekie, S.B. Poole, D.N. Payne: Electron. Lett. **21**, 738 (1985)

6. I.P. Alcock, A.C. Tropper, A.I. Ferguson,D.C. Harma: Electron. Lett. **22**, 84 (1986)
7. I.P. Alcock, A.I. Ferguson. D.C. Hanna, A.C. Tropper: Electron. Lett. **22**, 268 (1986)
8. G. Geister, R. Ulrich: Opt. Commun. **68**, 187 (1988)
9. I.N. Duling, L. Goldberg, J.F. Weller: Electron. Lett. **24**, 1333 (1988)
10. M.W. Phillips, A.I. Ferguson, D.C. Hanna: Opt. Lett. **14**, 219 (1989)
11. J.D. Kafka, T. Baer, D.W. Hall: Opt. Lett. **14**, 1269 (1989)
12. M.E. Fermann, M. Hofer, F. Haberl, S.P. Craig-Ryan: Electron. Lett. **26**, 1737 (1990)
13. M.E. Fermann, M. Hofer, F. Haberl, A.J. Schmidt, L. Turi: Opt. Lett. **16**, 244 (1991)
14. I.N. Duling: Opt. Lett. **16**, 539 (1991)
15. M.H. Ober, M. Hofer, M.E. Fermann: Opt. Lett. **18**, 367 (1993)
16. M. Hofer, M.E. Fermann, F. Haberl, M.H. Ober, A.J. Schmidt: Opt. Lett. **16**, 502 (1991)
17. R.L. Fork, B.I. Greene, C.V. Shank: Appl. Phys. Lett. **38**, 671 (1981)
18. P.F. Curley, C. Spielmann, T. Brabec, F. Krausz, E. Wintner, A.J. Schmidt: Opt. Lett. **18**, 54 (1993)
19. B.P. Nelson, K. Smith, K.J. Blow: Electron. Lett. **28**, 656 (1992)
20. E.J. Greer, K. Smith: Electron. Lett. **28**, 1741 (1992)
21. M.L. Stock, L.M. Yang, M.J. Andrejco, M.E. Fermann: Opt. Lett. **18**, 1529 (1993)
22. K. Smith, J.K. Lucek: Electron. Lett. **28**, 1814 (1992)
23. K. Smith, J.K. Lucek: OSA Conf. Lasers and Electro-Optics, CLEO, Baltimore (1993), paper CPD23
24. S.V. Chernikov, J.R. Taylor, P.V. Mamyshev, E.M. Dianov: Electron. Lett. **28**, 931 (1992)
25. M. Nakazawa, K. Suzuki, Y. Kimura: Opt. Lett. **15**, 715 (1990)
26. A. Galvanauskas, A. Krotkus, J.A. Tellefsen, M. Öberg, B. Broberg: Electron. Lett. **27**, 2394 (1991)
27. M. Zirngibl, L.W. Stulz, J. Stone, J. Hugi, D. DiGiovanni, P.B. Hansen: Electron. Lett. **27**, 1734 (1991)
28. W.H. Loh, D. Atkinson, P.R. Morkel, M. Hopkinson, A. Rivers, D.N. Payne: IEEE Photon. Technol. Lett. **5**, 35 (1993)
29. H. Takara, S. Kawanishi, M. Saruwatari, K. Noguchi: Electron. Lett. **28**, 2095 (1992)
30. A. Takada, H. Miyazawa: Electron. Lett. **26**, 217 (1990)
31. D.J. Kuizenga, A.E. Siegmann: IEEE J. QE-**6**, 694 (1970)
32. W.J. Miniscalco, L.J. Andrews, B.A. Thompson, T. Wei, B.T. Hall: In *Fiber Laser Sources and Amplifiers*, SPIE Proc. **1171**, 93 (1989)
33. F. Krausz, T. Brabec, E. Wintner, A.J. Schmidt: Appl. Phys. Lett. **55**, 2386 (1990)
34. M. Hofer, M.E. Fermann, F. Haberl, J.E. Townsend: Opt. Lett. **15**, 1467 (1990)
35. H.A. Haus, Y. Silberberg: IEEE J. QE-**22**, 325 (1986)
36. K. Smith, J.R. Armitage, R. Wyatt, N.J. Doran, S.M.J. Kelly: Electron. Lett. **26**, 1149 (1990)
37. S.M.J. Kelly, K. Smith, K.J. Blow, N.J. Doran: Opt. Lett. **16**, 1337 (1991)
38. K.J. Blow, N.J. Doran, B.K. Nayar, B.P. Nelson: Opt. Lett. **15** 248 (1990)
39. O.E. Martinez, R.L. Fork, J.P. Gordon: J. Opt. Soc. Am. B **2**, 753 (1985)
40. P. A. Belanger, L. Gagnon, C. Pare: Opt. Lett. **14**, 943 (1989)
41. H.A. Haus, J.G. Fujimoto, E.P. Ippen: J. Opt. Soc. Am. B **8**, 2068 (1991)
42. H.A. Haus, E.P. Ippen, K. Tamura: Additive Pulse Mode locking in Fiber Lasers. IEEE J. QE (to be published)
43. T. Brabec, C. Spielmann, F. Krausz: Opt. Lett. **16**, 1961 (1991)
44. T. Brabec, C. Spielmann, F. Krausz: Opt. Lett. **17**, 748 (1992)
45. F. Krausz, M.E. Fermann, T. Brabec, P.F. Curley, M. Hofer, M.H. Ober, C. Spielmann, E. Wintner, A.J. Schmidt: IEEE J. QE-**28**, 2097 (1992)
46. M. E. Fermann, F. Haberl, M. Hofer, H. Hochreiter: Opt. Lett. **15**, 752 (1990)
47. D. Mortimer: J. Light. Technol. LT-**6**, 1217 (1988)
48. N.J. Doran, D. Wood: Opt. Lett. **13**, 56 (1988)
49. M.E. Fermann, M. Hofer: Europ. Conf. on Optical Communication, ECOC 91, and Int'l Conf. on Integrated Optics and Optical Communication IOOC 91, Paris (1991) paper TuB4.2
50. R.H. Stolen, J. Botineau, A. Ashkin: Opt. Lett. **7**, 512 (1982)
51. H. Winful: Appl. Phys. Lett. **47**, 213 (1985)
52. M. Hofer, M.H. Ober, F. Haberl, M.E. Fermann: IEEE J. QE-**28**, 720 (1992)
53. F. Krausz, T. Brabec, C. Spielmann: Opt. Lett. **16**, 235 (1991)
54. H.A. Haus, E.P. Ippen: Opt. Lett. **16**, 1331 (1991)
55. F. Krausz, T. Brabec: Opt. Lett. **18**, 888 (1993)
56. V.J. Matsas, T.P. Newson, D.J. Richardson, D.N. Payne: Electron. Lett. **28**, 1391 (1992)
57. K. Tamura, J. Jacobson, E.P. Ippen, H.A. Haus, J.G. Fujimoto: Opt. Lett. **18**, 220 (1993)
58. M. Nakazawa, E. Yoshida, T. Sugawa, Y. Kimura: Electron. Lett. **29**, 1327 (1993)
59. M.E. Fermann, M.J. Andrejco, Y. Silberberg. M.L. Stock: Opt. Lett. **18**, 894 (1993)
60. M.E. Fermann, M.J. Andrejco, M.L. Stock, Y. Silberberg, A. M. Weiner: Appl. Phys. Lett. **62**, 910 (1993)
61. M.E. Fermann, L.M. Yang, M.L. Stock, M.J. Andrejco: Opt. Lett. **19**, 43 (1994)
62. I.N. Duling, R.D. Esnam: Electron. Lett. **28**, 1126 (1992)
63. D. Taverner, D.J. Richardson, D.N. Payne: OSA Technol. Digest Ser. **15**, 367 (1993)
64. A. Grudinin, D.J. Richardson, D.N. Payne: Electron. Lett. **28**, 1391 (1992)
65. V.J. Matsas, W.H. Loh, D.J. Richardson: IEEE Photon. Lett. **5**, 492 (1993)
66. I.N. Duling: Role of Dispersion in limiting pulse widths in fiber lasers. Appl. Phys. Lett. (to be published)
67. J.P Gordon: J. Opt. Soc. Am. B **9**, 91 (1992)
68. S.M.J. Kelly: Electron. Lett. **28**, 806 (1992)
69. M.E. Fermann, M. Hofer, F. Haberl, A.J. Schmidt: Europ. Conf. Optical Communication, Amsterdam (1990) p. 1053
70. D.J. Richardson, R.I. Laming, D.N. Payne, M.W. Phillips, V.J. Matsas: Electron. Lett. **27**, 730 (1991)
71. N. Pandit, D.U. Noske, S.M.J. Kelly, J.R. Taylor: Electron. Lett. **28**, 455 (1992)
72. M. Hofer: Ultrashort pulse generation in optical fiber lasers. Dissertation, Technical University of Vienna (1992)
73. M. Hofer, M.H. Ober, F. Haberl, M.E. Fermann, E.R. Taylor, K.P. Jedrezejewski: Opt. Lett. **17**, 807 (1992)
74. K. Tamura, E.P. Ippen, H.A. Haus, L.E. Nelson: Opt. Lett. **18**, 1080 (1993)
75. W.J. Tomlinson, R.H. Stolen, C.V. Shank: J. Opt. Soc. Am. B **1**, 139 (1984)
76. M.H. Ober, F. Haberl, M.E. Fermann: Appl. Phys. Lett. **60**, 2177 (1992)
77. G.T. Harvey, L.F. Mollenauer: OSA Technol. Digest. Ser. **12**, 318 (1992)
78. E. Yoshida, Y. Kimura, M. Nakazawa: Appl. Phys. Lett. **60**, 932 (1992)
79. M.L. Dennis, I.N. Duling: Electron. Lett. **28**, 1894 (1992)
80. A.B. Grudinin, D.J. Richardson, D.N. Payne: Electron. Lett. **29**, 1860 (1993)
81. E.M. Dianov, A.V. Luchnikov, A.N. Pilipetskii, A.M. Prokhorov: Appl. Phys. B **54**, 175 (1992)
82. E A. DeSouza, M.N. Islam, C.E. Soccolich, W. Pleibel, R.H. Stolen, J.R. Simpson, D.J. DiGiovanni: Electron. Lett. **29**, 447 (1993)
83. M.H. Ober, M. Hofer, T.H. Chiu, U. Keller: Opt. Lett. **18**, 1532 (1993)
84. P.W. Smith, Y. Silberberg, D.A.B. Miller: J. Opt. Soc. Am. B **2**, 1228 (1985)
85. H.A. Haus, Y. Silberberg: Opt. Soc. Am. B **2**, 1237 (1985)
86. M.N. Islam, E.R. Sunderman, C.E. Soccolich, I. Bar-Joseph, N. Sauer, T.Y. Chang, B.I. Miller: IEEE J. QE-**25**, 2454 (1989)
87. U. Keller, L.E. Nelson, T.H. Chiu: OSA Technol. Digest. Ser. **13**, 94 (1992)

88. U. Keller, D.A.B. Miller, G.D. Boyd, T.H. Chiu, J.F. Ferguson, M.T. Asom: Opt. Lett. **17**, 505 (1992)
89. M.E. Fermann: Unpublished data
90. M.E. Fermann, D.C. Hanna, D.P. Shepherd, P.J. Suni, J.E. Townsend: Electron. Lett. **24**, 894 (1988)
91. M.E. Fermann, M.L Stock, L.M. Yang, M.J. Andrejco, D. Harter: OSA Technol. Digest. Ser. **15**, 329 (1993)
92. S.V. Chernikov, D.J. Richardson, R.I. Laming, E.M. Dianov, D.N. Payne: Electron. Lett. **28**, 1210 (1992)
93. E.M. Dianov, P.V. Mamyshev, A.M. Prokhorov, S.V. Chernikov: Opt. Lett. **14**, 1008 (1989)
94. P.V. Mamyshev, S.V. Chernikov, E.M. Dianov: IEEE J. QE-**27**, 2347 (1991)
95. S.V. Chernikov, J.R. Taylor: Electron. Lett. **29**, 658 (1993)
96. A.M. Weiner, D.E. Leard: Opt. Lett. **15**, 51 (1990)
97. D. Burns, W. Sibbett: Electron. Lett. **26**, 505 (1990)
98. C.R.Ó. Cochláin, R.J. Mears, G. Sherlock: IEEE Photon. Technol. Lett. **5**, 25 (1993)
99. E.M. Dianov, T.R. Martirosian, O.G. Okhotnikov, V.M. Paramarov, A.M. Prokhorov: OSA Technol. Digest. Ser. **4**, 236 (1993)
100. L.F.Mollenauer, B.M. Nyman, M.J. Neubelt, G. Raybon, S.G. Evangelides: Electron. Lett. **27**, 178 (1991)
101. H.F. Liu, S. Oshiba, Y. Ogawa, Y. Kawai: Opt. Lett. **17**, 64 (1993)
102. A. Galvanauskas, P. Blixt, J.A. Tellefsen: Appl. Phys. Lett. **63**, 1742 (1993)
103. D. Strickland, G. Mourou: Opt. Commun. **56**, 219 (1985)
104. M.L. Stock, A. Galvanauskas, M.E. Fermann, G. Mourou, D. Harter: OSA Technol. Digest. Ser. **15**, (1993) paper PDP5